Journal of Porous Materials 7, 125–130 (2000)

Electro-, Photo- and Scanning Tunneling—Luminescence Studies of Efficient Light-Emitting Porous Silicon

V.A. KUZNETSOV, I. ANDRIENKO AND D. HANEMAN
School of Physics, University of New South Wales, Sydney 2052, Australia

Abstract. Porous silicon films as used in efficient blue-green electroluminescent devices (internal efficiency about 0.1%) were studied by scanning tunneling microscopy light emission spectroscopy (STMLES) as well as photoluminescence (PL) and electroluminescence (EL) spectroscopy. Areas of the n-type porous Si surfaces with small particles of about 5 nm dimensions gave STMLE, but areas with larger structures gave no emission. Clear STMLE spectra gave a peak at 630 nm, quite different from the EL peak at 500 nm. Whereas the PL peak at 700 nm was consistent with the STM indication of quantised entities, the EL seemed more readily explicable in terms of defects at the metal contact barrier.

Keywords: porous silicon, photoluminescence, electroluminescence, scanning tunneling microscopy

I. Introduction

The fabrication of porous silicon, although relatively straightforward, is extremely sensitive to details of anodising conditions and also mode of handling after removal from the bath [1]. The most practical applications of the material are in fabrication of efficient electroluminescent devices, in which area of development much success has been reported recently [2–8], based not only on scientific understanding but also on trials of various fabrication parameters. The occurrence of EL and PL at energies much greater than the band gap of bulk Si, and the efficiencies of emission having values much greater than the normal bulk-band radiative recombination, have been explained in various ways. However, there is a large accumulation of evidence favouring an explanation of most of the PL in terms of quantum confined columns or particles [1].

There has been relatively little direct evidence of the existence of structures having the necessarily small dimensions of a few nm, mostly from transmission electron microscopy. For topography, scanning electron microscopy, (SEM), generally gives poor images, although it was shown that heat treatment of films could cause improved definition of structures, clearly showing spheroidal particles down to about 15 nm dimensions [9]. However, the best SEM resolution is still generally above the quantum confinement range of a few nm. STM is capable of sufficient resolution, and some studies have been published for porous Si (summarised in [1]), but none on films that have been shown to be useful in the desired EL devices.

In this work we have fabricated EL devices that function quite efficiently in the blue-green range, a desired region of emission, and studied such films both by normal topographic STM, and by the detection and spectral measurement of light emission during electron tunneling. Such techniques have been previously applied to por-Si [10–14] but with limited signal/noise, and not to device-effective material.

II. Porous Layer and Device Preparation

The silicon wafers to be anodised were n-type of 0.005–0.020 ohm cm resistivity, 0.52 mm thick, with (1 1 1) surfaces, and having an oxide layer on the back side. This side then had part of its oxide layer removed by immersing part of the surface in a 27% HF solution for a few seconds. The new surface was anodised in a 1% HF aqueous solution for 7 min at a current density of 3 mA cm^{-2}, this being a so-called transition regime [7], just below the electropolishing regime of 4 mA cm^{-2} and higher. To aid hole formation, the surface was illuminated with light from a 100 W tungsten

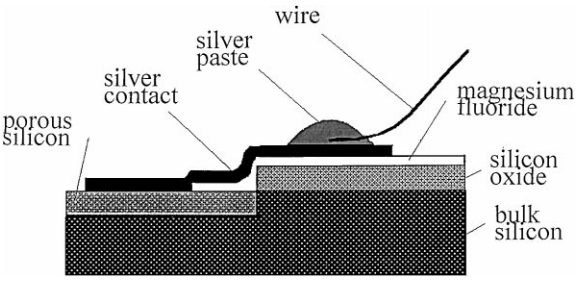

Figure 1. Schematic structure of construction of the Schottky barrier por-Si device. Emission is through the silver contact film.

filament bulb distant 10 cm from the sample at an angle close to normal. The wafer was lifted from the solution and washed with a mild jet of absolute ethanol, followed by a weak stream of air. The porous silicon (por-Si) layer was examined visually and placed under an ultra violet lamp to check uniformity of PL. Films generally showed fairly uniform PL. The sample was forthwith placed in a vacuum chamber and evacuated to 5×10^{-5} Torr for deposition of a protective insulating layer of magnesium fluoride covering the interface between the por-Si and the remaining silicon oxide layer and also the latter. The vacuum chamber was reloaded and re-evacuated, and a semi-transparent silver film was deposited on the por-Si and MgF_2 layers through a shadow mask. Contact to the Ag layer was achieved by placing a small amount of silver paste onto the portion of film over the MgF_2 layer, and attaching a fine wire. If silver paste contacted the silver film over the por-Si, it invariably destroyed the device. The device structure is shown in Fig. 1. Note that emission is detected through the top silver film.

III. Electrical Measurements

EL was produced at room temperature in air under stimulation from electrical pulses of up to 40 V, with pulse periods of 20 ms and duty cycles from 1 : 100 to 1 : 1. The device lifetimes were reduced at the higher duty cycles. Total light output was measured with a Si detector (response 400–1050 nm) and a Ge detector (response 800–1700 nm). Visible-range spectral measurements were performed with a set of optical filters covering the range 400–700 nm, each with a half-peak bandwidth of 60 nm, and the results corrected for detector response and filter transmission. Similar filter procedures were used for the infra-red light recorded by the Ge detector. The emission was imaged with a liquid nitrogen cooled CCD camera.

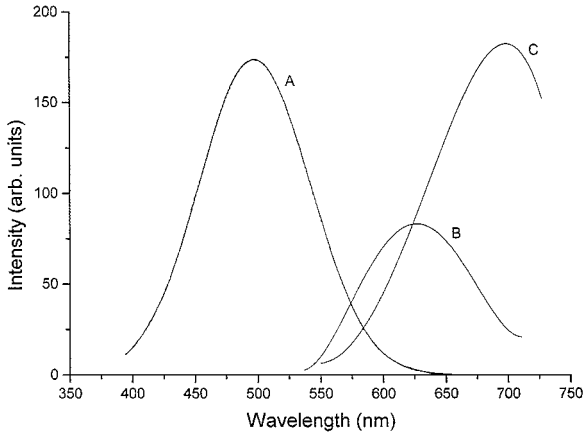

Figure 2. Curve A, spectrum of EL from por-Si device; B, spectrum of STM light emission; C, spectrum of PL from same por-Si film.

IV. Device Performance

The devices exhibited EL only in reverse bias, and for structures that had good rectification ratios, up to 1000. The intensity of EL was approximately linear with current. The EL registered with the Si detector became observable at a current density above 0.02 mA cm^{-2}, (at 10 V) but with the Ge detector the current density needed to be above about 1 mA cm^{-2} (at 20 V).

The EL spectrum is shown in Fig. 2 and was measured at a current density of 1 mA cm^{-2}, just below the onset of Ge-detectable emission. With pulse widths of 0.2 ms and low duty cycles, the emission lasted only a few tens of seconds. Variations in duty cycle and pulse widths did not affect the spectrum. The infra-red spectrum showed a distribution with a peak at 1100 nm and is presumably mainly due to recombination across the bulk Si band gap.

To obtain longer lifetimes, some organic encapsulation methods were tried, but preliminary work was not successful. However when the device was mounted in a vacuum chamber at 10^{-3} Torr, it emitted light for about an order of magnitude longer. Such improvements have been noted before [4]. Presumably the heat developed during passage of current promotes degradation of the por-Si structure by interaction with the atmosphere. Even in vacuum there is still gas trapped in the por-Si layer which can cause deleterious effects when heat occurs.

If the radiation is approximately isotropic, the internal efficiency was calculated to be 0.1% in the Si detector range, and 4 times higher in the Ge detector range.

After application of a square pulse of 20 V, the mainly visible emission recorded with the Si detector

decayed to about one third in 3–10 μs, similar to times found previously [8], whereas the mainly infra-red light recorded with the Ge detector showed a decay time of 50–100 μs. This demonstrates that the two emission regions have different origins.

V. STM and STMLES Measurements

For STM topographic surveys, the por-Si surfaces were produced as above, and mounted at once (without any coatings) in the STM vacuum system. The STM head was a Burleigh ARIS-4400 unit. A vacuum of 10^{-8} Torr was obtained, with no bakeout of the chamber. Electrochemically etched Pt-Ir tips were used. Best imaging conditions were with a tip voltage numerically smaller than -5 V, and current of 1 nA. Many areas covered by small lumps were noted. An example is shown in Fig. 3. Porous regions appear usually on only part of large-scale STM scans. This may be an effect related to scanning methods. A higher magnification area displaying small, 2–4 nm, hillocks is shown in Fig. 4.

Tunneling of electrons from the tip into excited states in the sample can occur, and these excited states can relax by at least some radiative processes. Such light emission has been detected from several kinds of surface [13, 14]. For such an experiment, a lens was mounted on the STM frame with its focus at the scanning tip. Light generated at the tip region passed through a window in the vacuum system and was focussed onto the entrance slit of a prism spectrograph as shown in Fig. 5. The spectrum appeared on a liquid-nitrogen cooled CCD image plate. The visible range 450–720 nm could be measured.

The best size areas for obtaining satisfactory spectra were of dimensions 10–13 nm. A typical area from which light was recorded is shown in Fig. 4. Further reduction in scan size rendered the light too weak. Reports of light emission from single particles have shown poor signal/noise ratio with some uncertainty about the emission peak [13, 14]. The spectra we obtained were quite clear, as shown in Fig. 6. The STMLE spectrum in this figure was obtained by binning the 512 pixel width on the CCD image plate into 8 bin units. The scanning time was 5 min, in which time the tip drift was 3.5 nm, so the majority of the 10 or 13 nm square area shown was scanned. The tunneling conditions for light emission were 25–90 nA and -7 to -9 V. The spectrum did not depend on tunneling current as shown in Fig. 7. However, higher voltages and currents damaged the surface, with hollows appearing on the surface.

These appear to be the first STMLE studies of n-type por-Si. The spectra could be obtained under bias conditions as low as -7 V and 25 nA, much lower than some conditions reported previously, namely -50 V and 100 nA [12].

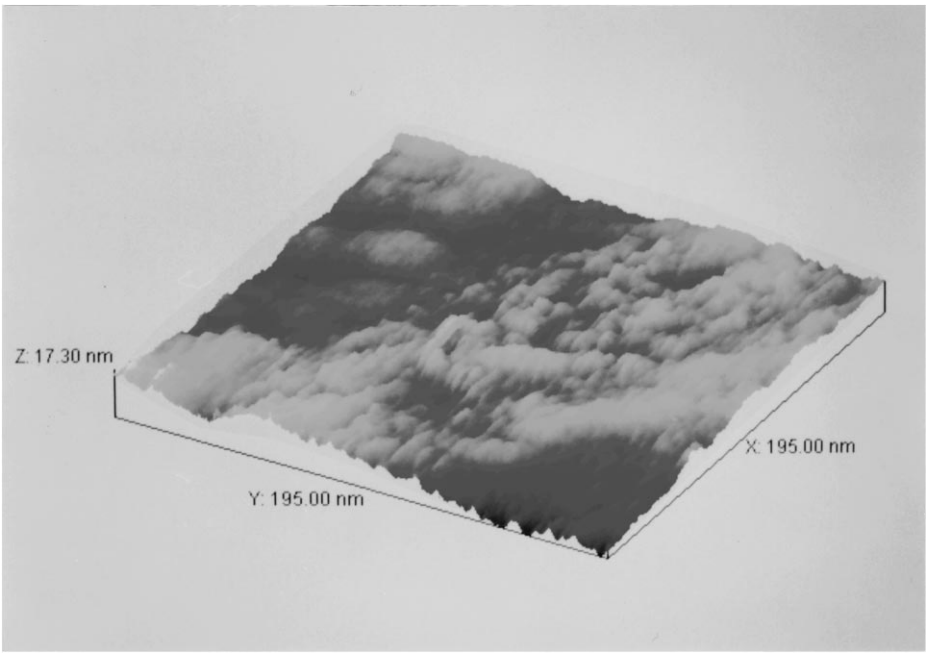

Figure 3. STM topographic scan of por-Si surface. Scan area is 195 nm square.

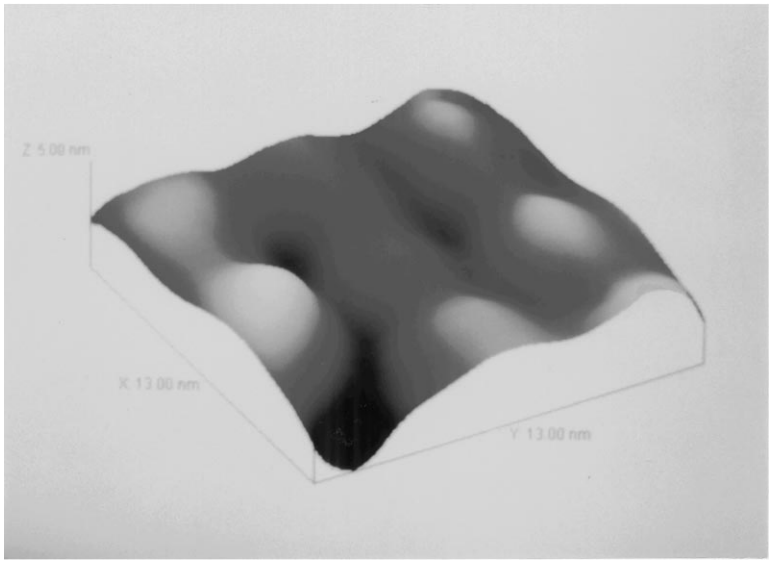

Figure 4. STM topographic scan of por-Si surface. Scan area is 13 nm square.

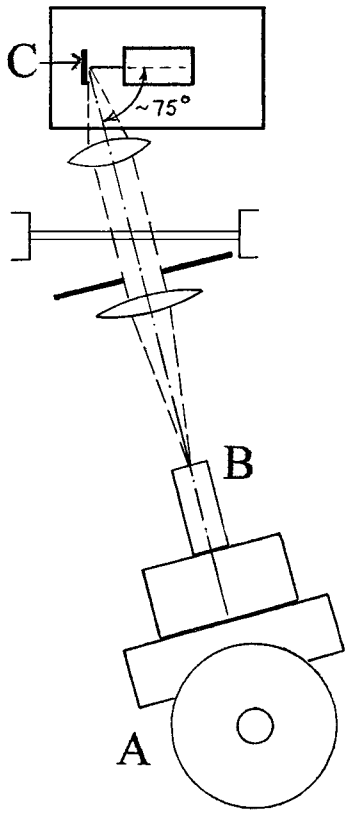

Figure 5. Schematic diagram of apparatus for measuring spectra of light emission from STM tunneling region. A, liquid-nitrogen cooled CCD camera; B, prism spectrograph; C, specimen.

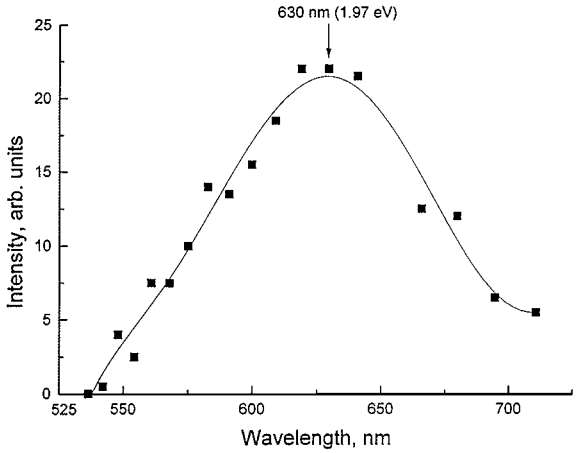

Figure 6. Original data from STMLE scan of por-Si area of 13 nm square. The 512 pixel width of the CCD array was divided into bins of 8 pixels to improve signal/noise ratio. The CCD dark counts have been subtracted. Tip voltage, −7.0 V, tunneling current 90.2 nA.

Light was emitted only from areas covered by very small particles or protrusions. No other areas gave emission. This is consistent with the quantum confinement model of light emision.

The same arrangement was used to measure PL from the surfaces studied by STMLE. The 435.8 nm light from a high pressure mercury discharge lamp illuminated the sample and PL was detected by the spectrograph and CCD plate. The spectrum is shown in Fig. 2. The peak occurs at 700 nm (1.77 eV).

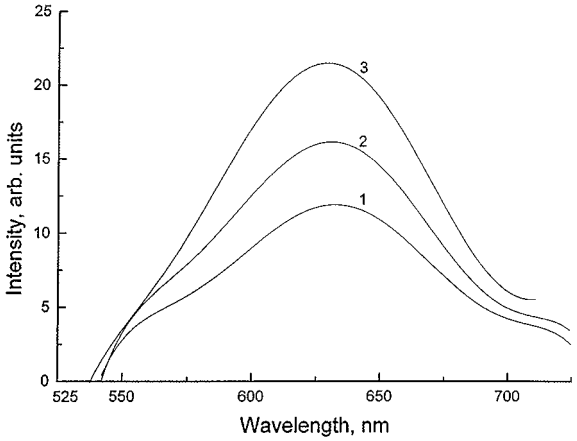

Figure 7. Dependence of spectrum of STM light emission from por-Si on tunneling current I. Data have been smoothed. Curve 1, $I = 25.3$ nA. Curve 2, $I = 50.1$ nA. Curve 3, $I = 90.2$ nA. Scan area 13 nm square. Tip voltage -7.0 V.

VI. Discussion

Reference to the spectra in Fig. 2 shows that the PL and STMLE peaks occur at similar but not identical wavelengths, namely 700 and 630 nm respectively. The EL peak occurs at a significantly shorter wavelength of 500 nm. Relatively small differences between PL and STM spectra are not unusual [13, 14]. The PL spectrum is excited by light from depths of fractions of a micron whereas the STM spectrum is excited by electron injection at the very surface of the film, where the particles are often slightly smaller than the distribution underneath, which gives the PL spectrum. Such size distributions are known to occur [1].

If the EL spectrum peaking at 500 nm (2.48 eV) is due to quantum confinement, it would require particle sizes in the region of less than 2 nm [15]. The STM observations do not find much evidence for such small particles. Hence the radiation is probably too far in the blue for quantum confinement to be significantly involved. The EL may arise from a different source, namely carrier recombination at centers formed on portions of the por-Si near the Schottky barrier with the top evaporated metal film. The difference in luminescence decay times between the bulk Si infra-red emission and the EL is consistent with the view that a different origin is involved. The recombination centers could occur in Si oxides [8] or hydrides. An origin near the metal contact is consistent with our finding that when the devices had deteriorated and finished emitting blue-green light, in some cases there were several dots of white emission which continued to be active, presumably from the underlying porous layer.

The strong infra-red emission peaked around the Si band-gap is probably recombination in Si cores which are not quantum confined, but still small enough to reduce non-radiative recombination at defects and by Auger processes, as has been discussed [16].

The EL appeared to be non-uniform, and occurred in many dots of high brightness, which implied that there were non-uniform effects on the surface of the film. This may be the non-uniform film created by our procedures, and or non-uniformities in the metal contact.

VII. Conclusions

We have described the fabrication and operation of an efficient (internal efficiency about 0.1%) por-Si device emitting through the top contact in the blue-green region of the spectrum. The method uses white light illumination during anodising. Scanning tip light emission studies of the porous layer found emission at wavelengths similar to those of PL, but not EL, and it is concluded that the latter is mainly due to sources other than quantum confinement, probably involving hydrides or oxides at the Schottky barrier contact region. In common with general experience with por-Si, the devices quickly deteriorated in air, and proper encapsulation techniques would be required for extended lifetimes.

Acknowledgment

This work was supported by the Australian Research Council.

References

1. A.G. Cullis, L.T. Canham, and P.D. Calcott, J. Appl. Phys. **82**, 909 (1997).
2. S. Lazarouk, P. Jaguiro, S. Katsouba, S. LaMonica, G. Magiello, G. Masini, and A. Ferrari, Thin Solid Films **276**, 168 (1996).
3. J. Linnros and N. Lalic, Appl. Phys. Lett. **66**, 3048 (1995).
4. A. Loni, A.J. Simons, T.I. Cox, P.D.J. Calcott, and L.T. Canham, Electronics Lett. **31**, 1288 (1995).
5. H. Mimura, T. Matsumoto, and Y. Kanemitsu, J. Non-Cryst. Solids **198–200**, 961 (1996).
6. P. Steiner, F. Kozlowski, M. Wielunski, and W. Lang, Jpn. J. Appl. Phys. **33**, 6075 (1994).
7. M. Bertolotti, F. Carassiti, E. Fazio, A. Ferrari, S. LaMonica, S. Lazarouk, G. Liakhou, G. Maiello, E. Proverbio, and L. Schirone, Thin Solid Films **253**, 152 (1995).

8. G.G. Qin, Y.M. Huang, J. Lin, L.Z. Zhang, and B.R. Zhang, Solid State Commun. **94**, 607 (1995).
9. R. Sabet-Dariani and D. Haneman, J. Appl. Phys. **76**, 1346 (1994).
10. Ph. Dumas, M. Gu, C. Syrykh, J.K. Gimzewski, I. Makarenko, A. Halimaoui, and F. Salvan, Europhys. Lett. **23**, 197 (1993).
11. M. Gu, C. Syrykh, A. Halimaoui, Ph. Dumas, and F. Salvan, J. Lumin. **57**, 315 (1993).
12. Ph. Dumas, M. Gu, C. Syrykh, A. Halimaoui, F. Salvan, J.K. Gimzewski, and R.R. Schlittler, J. Vac. Sci. Tech. **B12**, 2064 (1994).
13. K. Ito, S. Ohyama, Y. Uehara, and S. Ushioda, Appl. Phys. Lett. **67**, 2536 (1995).
14. S. Ushioda, Appl. Surf. Sci. **113/114**, 335 (1997).
15. B. Delley and E.F. Steigmeier, Appl. Phys. Lett. **67**, 2370 (1995).
16. D. Haneman and J. Yuan, Appl. Surf. Sci. **113/114**, 103 (1997).